



LUND UNIVERSITY

Thin InAs membranes and GaSb buffer layers on GaAs(001) substrates

Astromskas, Gvidas; Borg, Mattias; Wernersson, Lars-Erik

Published in:
Journal of Vacuum Science and Technology B

DOI:
[10.1116/1.4739425](https://doi.org/10.1116/1.4739425)

2012

[Link to publication](#)

Citation for published version (APA):
Astromskas, G., Borg, M., & Wernersson, L.-E. (2012). Thin InAs membranes and GaSb buffer layers on GaAs(001) substrates. *Journal of Vacuum Science and Technology B*, 30(5), Article 051202.
<https://doi.org/10.1116/1.4739425>

Total number of authors:
3

General rights

Unless other specific re-use rights are stated the following general rights apply:
Copyright and moral rights for the publications made accessible in the public portal are retained by the authors and/or other copyright owners and it is a condition of accessing publications that users recognise and abide by the legal requirements associated with these rights.

- Users may download and print one copy of any publication from the public portal for the purpose of private study or research.
- You may not further distribute the material or use it for any profit-making activity or commercial gain
- You may freely distribute the URL identifying the publication in the public portal

Read more about Creative commons licenses: <https://creativecommons.org/licenses/>

Take down policy

If you believe that this document breaches copyright please contact us providing details, and we will remove access to the work immediately and investigate your claim.

LUND UNIVERSITY

PO Box 117
221 00 Lund
+46 46-222 00 00

Thin InAs membranes and GaSb buffer layers on GaAs(001) substrates

Gvidas Astromskas, Mattias Borg, and Lars-Erik Wernersson

Citation: *J. Vac. Sci. Technol. B* **30**, 051202 (2012); doi: 10.1116/1.4739425

View online: <http://dx.doi.org/10.1116/1.4739425>

View Table of Contents: <http://avspublications.org/resource/1/JVTBD9/v30/i5>

Published by the AVS: Science & Technology of Materials, Interfaces, and Processing

Related Articles

Charge trapping analysis of Al₂O₃ films deposited by atomic layer deposition using H₂O or O₃ as oxidant
J. Vac. Sci. Technol. B **31**, 01A101 (2013)

MnP nanoclusters embedded in GaP epitaxial films grown by organometallic vapor-phase epitaxy: A reciprocal space mapping and transmission electron microscopy study
J. Vac. Sci. Technol. A **30**, 061510 (2012)

Atomic layer deposition of anatase TiO₂ on porous electrodes for dye-sensitized solar cells
J. Vac. Sci. Technol. A **31**, 01A116 (2013)

Effect of the amido Ti precursors on the atomic layer deposition of TiN with NH₃
J. Vac. Sci. Technol. A **31**, 01A117 (2013)

Crystal AlN deposited at low temperature by magnetic field enhanced plasma assisted atomic layer deposition
J. Vac. Sci. Technol. A **31**, 01A114 (2013)

Additional information on *J. Vac. Sci. Technol. B*

Journal Homepage: <http://avspublications.org/jvstb>

Journal Information: http://avspublications.org/jvstb/about/about_the_journal

Top downloads: http://avspublications.org/jvstb/top_20_most_downloaded

Information for Authors: http://avspublications.org/jvstb/authors/information_for_contributors

ADVERTISEMENT

<p>AVS 59th International Symposium & Exhibition</p> <p>October 28–November 2, 2012 • Tampa, Florida</p>	
 <p>212-248-0200 avsnyc@avs.org www.avs.org</p>	
<p>DIVISION/GROUP PROGRAMS:</p> <ul style="list-style-type: none"> • Advanced Surface Engineering • Applied Surface Science • Biomaterial Interfaces • Electronic Materials & Processing • Magnetic Interfaces & Nanostructures • Manufacturing Science & Technology • MEMS & NEMS • Nanometer-Scale Science & Technology • Plasma Science & Technology • Surface Science • Thin Film • Vacuum Technology 	<p>FOCUS TOPICS:</p> <ul style="list-style-type: none"> • Actinides & Rare Earths • Biofilms & Biofouling: Marine, Medical, Energy • Biointerphases • Electron Transport at the Nanoscale • Energy Frontiers • Exhibitor Technology Spotlight • Graphene & Related Materials • Helium Ion Microscopy • <i>InSitu</i> Microscopy & Spectroscopy • Nanomanufacturing • Oxide Heterostructures-Interface Form & Function • Scanning Probe Microscopy • Spectroscopic Ellipsometry • Transparent Conductors & Printable Electronics • Tribology

Thin InAs membranes and GaSb buffer layers on GaAs(001) substrates

Gvidas Astromskas and Mattias Borg

Solid State Physics, Lund University, Box 118, Lund SE-22100, Sweden

Lars-Erik Wernersson^{a)}

Electrical and Information Technology, Lund University, Box 118, Lund SE-22100, Sweden

(Received 12 April 2012; accepted 9 July 2012; published 26 July 2012)

Thin InAs layers and membranes are fabricated on GaAs substrates using GaSb buffer layers grown by MOVPE. The quality of the GaSb buffer layers is optimized and epitaxial InAs layers are grown on GaSb layers of various thickness. The best GaSb buffer layers are obtained for a nucleation temperature of 450 °C and a subsequent growth temperature of 570 °C with a V/III ratio of 3, as confirmed by both the structural (high-resolution XRD, AFM) and electrical (Hall) measurements. Furthermore, a clear relationship between the structural quality of the GaSb and InAs layers is established. Finally, free-standing InAs structures are fabricated where Hall measurements reveal a mobility that depends on the film thickness. © 2012 American Vacuum Society. [http://dx.doi.org/10.1116/1.4739425]

I. INTRODUCTION

The roadmap for the Si industry predicts a continued increase in the performance of the CMOS technology, although ultimately the scaling limits of the technology will make it difficult to further improve drive currents and maintain low leakage current densities. Both of these challenges can be remedied by using high-mobility III–V materials.¹ One such promising material is InAs, which has a high bulk electron mobility (30 000 cm²/V s). Already, high-performance InAs high electron mobility transistors have been demonstrated² as well as InAs- and InGaAs-based MOSFETs.^{3,4} These devices require integration of thin InAs layers onto insulating substrates. One option is to grow lattice-mismatched InAs/GaSb heterostructures on semi-insulating GaAs. The generation of misfit dislocation due to the very high lattice mismatch (7%) can be controlled by carefully adjusting the growth conditions for the GaSb buffer layer.^{5–7} However, this has so far required several micrometer thick buffer layers.⁸ Thick buffer layers are not attractive for electronic device integration as leakage currents and large height differences greatly complicate device design and fabrication. Therefore, we scale the thickness of the buffer layer and measure the relation between electrical and structural qualities of both the buffer and the top InAs layer. This way we investigate the quality requirements for a feasible integration of InAs onto lattice-mismatched substrates. As a first step toward advanced transistor architectures, we also etch the buffer and form free-standing InAs membranes that are evaluated electrically using the Hall bar technique.

This paper consists of three parts. First, we optimize the GaSb growth on GaAs(001) substrates in an MOVPE reactor, and characterize the quality of the grown GaSb layers. Second, we use the optimized GaSb buffers to deposit a thin layer of InAs. We vary the thickness of the GaSb buffer layer while the InAs layer is grown under the same conditions. The structural and electrical properties of both GaSb

and InAs layers are then evaluated and compared. Finally, we use the layers to fabricate free-standing InAs membranes that are characterized electrically.

II. EXPERIMENT

GaSb layers are grown using a horizontal reactor MOVPE system (Aixtron 200/4). TMIn, AsH₃, TMSb, and TEGa are used as precursors with hydrogen as a carrier gas with a total flow of 13 l/min. Semi-insulating and epi-ready GaAs(001) substrates were either directly loaded into the reactor or first cleaned by etching in 37% HCl for 3 min and rinsed in de-ionized water for 1 min. No significant improvement was observed for the etched samples. The GaSb buffer layers were grown using a two-step process, beginning with a nucleation step at low temperature followed by a buffer growth step at a higher temperature. To optimize the GaSb buffer layer, we varied the buffer growth temperature between 550 and 600 °C, the V/III ratio between 1 and 5, and the nucleation step temperature between 420 and 480 °C. It is verified by x-ray reflectometry and AFM measurements that the optimized nucleation step results in a rough 15-nm-thick layer. In the optimization series all GaSb layers were grown for 35 min, leading to a 1.3-μm-thick optimized GaSb layer. The growth rate was controlled *in situ* by reflectivity measurements.

Using optimized buffer growth conditions, 23- and 90-nm-thick InAs films were grown on GaSb buffers layers of various thicknesses. In order to obtain high quality hetero-interfaces, the growth temperature was lowered to 500 °C after the optimized GaSb buffer growth. An additional GaSb layer was grown for 1 min before switching to InAs, in order to switch between GaSb and InAs in a controlled manner. This was found to improve the FWHM value of the InAs 004 diffraction peak, as compared to switching without an intermediate low-temperature GaSb layer. The 23-nm-thick InAs layer was grown for 34 s at a growth temperature of 500 °C and a V/III ratio of 55, parameters which are known to give high-mobility InAs films.⁹ As 23 nm is below the critical thickness for the InAs/GaSb system, pseudomorphic

^{a)}Electronic mail: larserik.wernersson@eit.lth.se

InAs growth is expected. The grown samples were characterized by high-resolution x-ray diffraction (HR-XRD) measurements using a Bruker-AXS D8 system with a Cu $K\alpha$ x-ray source. Rocking curves and 2θ - ω scans of the 004 reflection were performed, as well as reciprocal space maps of the 224 reflection to evaluate the composition and strain. The FWHM of the 004 rocking curves, related to the mosaicity of a thin film, was used to compare the crystal quality in between different samples. Also, carrier mobility and concentration in the grown layers were measured using both Van der Pauw–Hall and Hall bar techniques, where contacts are formed by evaporating Ti/Au. The Hall measurements were performed at 0.18 T at both room temperature and 77 K.

III. RESULTS AND DISCUSSION

A. GaSb buffer optimization

The growth of GaSb buffer layers on GaAs substrates has been investigated by a few groups, but the growth conditions for high quality GaSb buffers are varying, indicating that a reactor specific growth optimization is required.^{6,7,10,11} Therefore, we first optimize the growth of relatively thick GaSb buffer layers (1.3 μm) with respect to nucleation temperature, growth temperature, and V/III ratio. On these samples, no InAs layers were grown, in order to focus the investigation on the structural quality of the GaSb buffer layer using HR-XRD, AFM, and Hall measurements.

All GaSb layers are found to be p type in the Hall measurements. The highest hole mobility and the sharpest HR-XRD peaks are obtained at a V/III ratio between 2 and 3.5 as shown in Fig. 1(b). A V/III ratio equal to 1.0 is detrimental for the GaSb growth, as confirmed by HR-XRD and Hall measurements. Under these conditions, a lack of Sb can cause the formation of Sb vacancies or even Ga droplets on the growth surface.⁶ The hole mobility of the GaSb layer decreases when the V/III ratio exceeds 4, although the FWHM of the 004 peak only increases slightly. A similar behavior is reported for GaSb grown from TMGa.⁷ The FWHM of the 004 rocking curve of the sample grown under a V/III ratio of 3 is measured to be 291 arcsec, while the sample grown under the V/III ratios of 4 and 5 show an FWHM of 320 and 318 arcsec, respectively.

A growth temperature of 570 °C is found to be optimal for growth of the GaSb buffer layers, as shown in Fig. 1(c). The crystal quality decreases for lower growth temperatures possibly due to a decrease in the adatom diffusion length, while the decrease at higher temperatures may be related to an increasing Sb desorption from the substrate; thus reducing the effective V/III ratio. A similar relation has previously been obtained for thicker buffer layers.⁸

A low-temperature nucleation step can be used when growing GaSb on GaAs substrates to relieve the strain caused by the high lattice mismatch between the two materials. We varied the nucleation step temperature between 420 and 480 °C as shown in Fig. 1(d) and observe the highest buffer layer quality when nucleation is performed at 450 °C. We note that the GaSb fully relaxes within the thickness of

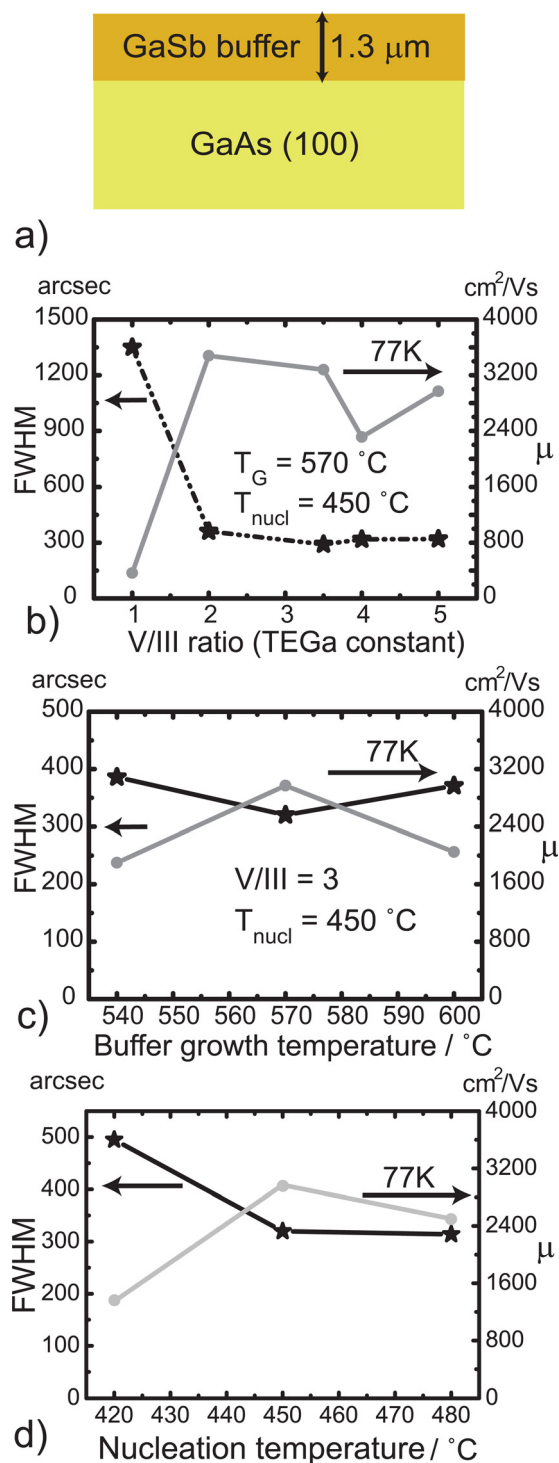


FIG. 1. (Color online) (a) Schematic illustration of a GaSb buffer layer grown on a GaAs(001) substrate. Structural and electrical quality of GaSb buffer layers as a function of (b) V/III ratio, (c) temperature during buffer growth, and (d) temperature during nucleation. The growth temperature (T_G), nucleation temperature (T_{nuc}), and V/III ratio were set to optimized values in each series.

the nucleation layer, as no residual strain is measured in the GaSb buffer layers by HR-XRD. The rms values of the surface roughness are presented in Table I, which show moderate surface rms values (~ 6 nm) for optimized 1.3 μm buffer layers. The nonoptimal rms values can be attributed to the presence of screw dislocations, visible in the AFM image of

TABLE I. Root-mean-square values of GaSb buffer layers.

Sample number	V/III	T_G (°C)	T_{nucl} (°C)	GaSb rms (nm)
2159	1	570	450	107
2157	2	570	450	8.4
2158	3.5	570	450	6.7
2165	4	570	450	6.42
2160	5	570	450	6.28
2161	5	600	450	4.22
2162	5	540	450	6.66
2163	5	570	420	23.7
2164	5	570	480	6.47

Fig. 3(a). Screw dislocations are observed in all samples with no clear relation between their density and growth parameters. This indicates that the improvement of the layer quality under optimized growth conditions is not related to a reduction in the density of screw dislocations for the densities observed here. We should also consider that the average spacing is much longer than the carrier scattering length observed in the electrical data. Instead, the improvement is most likely related to a reduction of threading dislocation density in the upper parts of the films. Possibly, using multiple nucleation steps in sequence could further improve the quality of the GaSb buffer layers, as demonstrated for InAs growth on Si(111).¹²

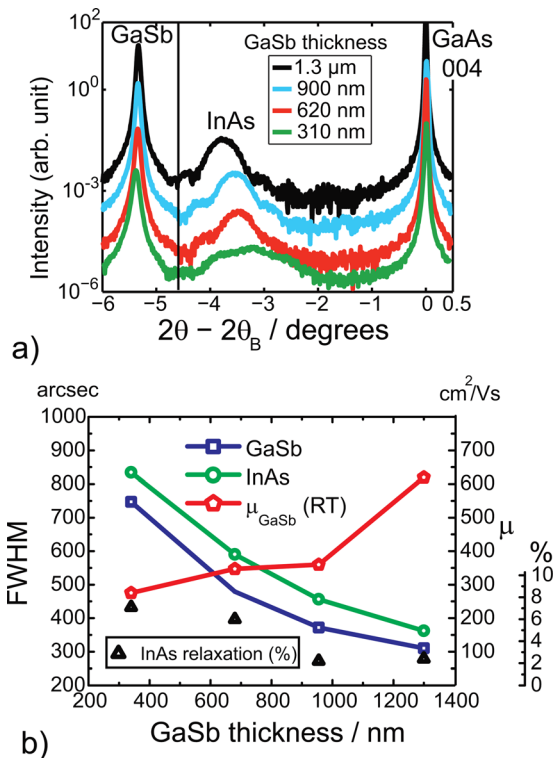


FIG. 2. (Color online) (a) 2θ - ω scans around the 004 reflection of InAs/GaSb structures with various GaSb thicknesses. The thickness of the InAs layer is 23 nm for all samples. Pendellösung fringes are observed for the InAs peak at larger buffer thicknesses. The vertical line indicates the position of fully strained InAs. (b) Structural and electrical properties of InAs/GaSb as a function of the GaSb layer thickness. The quality of the InAs layer is directly related to the GaSb buffer layer and the quality of the GaSb layer increases with the thickness.

B. Structural evaluation of InAs/GaSb heterostructures

In a second series of samples, thin layers of InAs were grown on top of the GaSb buffer layers. In order to correlate the quality of the GaSb buffer layer with the quality in the InAs layer, we varied the thickness of the GaSb buffer layer in the InAs/GaSb heterostructures and performed HR-XRD measurements on the structure. The thickness of the InAs layer was kept at 23 nm, which is below the critical thickness of the structure as calculated from People and Bean¹³ (36 nm). XRD 2θ - ω scans of InAs/GaSb samples with varying GaSb buffer thickness are compared in Fig. 2(a). Here, it is observed that the InAs peaks exhibit Pendellösung fringes for the samples with a buffer thickness above 620 nm, indicating a low roughness at the interface between GaSb and InAs. Also, the peak position of the InAs shifts toward lower 2θ values for the thicker buffer layers. A combination of HR-XRD measurements of the 004 and 224 reflections verifies that this shift is caused by a combination of reduced

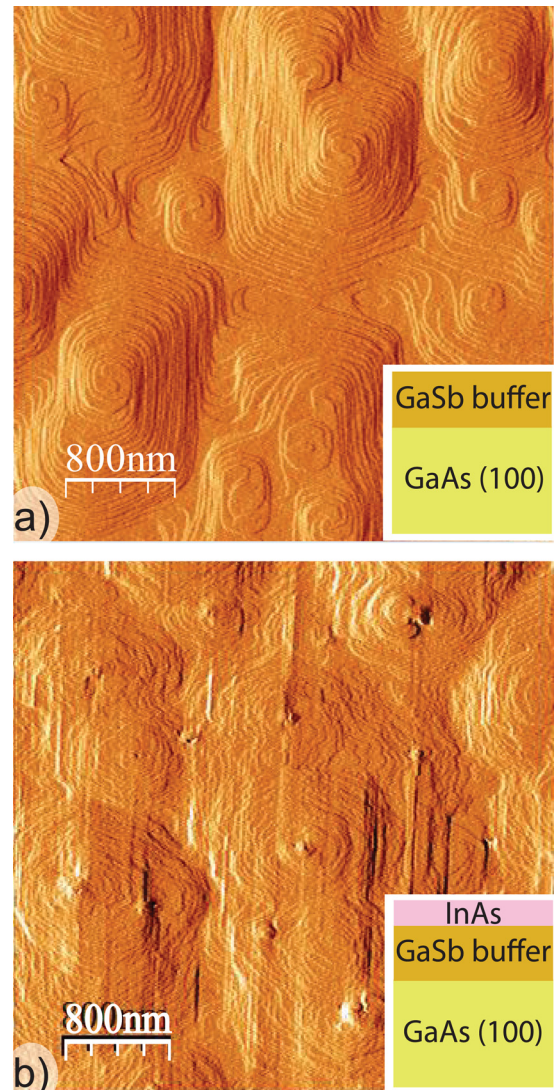


FIG. 3. (Color online) $4 \times 4 \mu\text{m}^2$ AFM images of (a) 300 nm optimized GaSb buffer layer, (b) InAs surface, grown on 1.3 μm GaSb buffer. The screw dislocations are clearly visible on the GaSb surface, while the InAs growth starts to mitigate them. Insets show schematic illustrations of the evaluated structures. The rms values are 4.35 and 5.93 nm for (a) and (b), respectively.

strain relaxation and a modification of the InAs composition due to a carryover of Ga and/or Sb.

The FWHM of the GaSb 004 rocking curve decreases as the GaSb buffer thickness increases, as shown in Fig. 2(b). Both the crystal and electrical quality are improving rapidly as the buffer thickness is increased to 1 μm . A clear correlation between the rocking curve FWHM of the GaSb buffer and the InAs is observed and the FWHM of the InAs layer follows the GaSb data, although with a roughly 100 arcsec wider peak. The quality of the thin InAs film thus appears to be directly dependent on the quality of the underlying GaSb buffer. The higher FWHM of the InAs is attributed to the strain in the InAs film, which is nearly pseudomorphic to the GaSb buffer in all cases.

Reciprocal space maps of the 224 reflection were obtained (not shown) in order to separate the influence of strain and composition. It was found that the InAs layer grown on a 310 nm GaSb buffer was 7% relaxed and had a Bragg peak that was significantly shifted from the position of bulk InAs. For GaSb buffer thickness exceeding 620 nm, the InAs film was only 2% relaxed, and the InAs peak position was closer to the position of bulk InAs. This indicates that the amount of relaxation and the amount of compositional carryover of Ga and Sb from GaSb into the InAs layer is related to the quality of the InAs and GaSb layers. Previously, Ga carryover in the InAs(Sb)/GaSb system has been reported by Lackner *et al.*,¹⁴ where it was found not to be an effect of the gas switching, but rather due to adsorbed Ga. The Ga carryover may be aggravated in our case, as the comparably high dislocation density present in the thin GaSb buffers may present additional adsorption sites for Ga. It is also likely that there are a few percent of Sb carried over into the InAs layer, due to the well-known segregation effect of Sb.¹⁵ Incorporation of Sb and Ga would move the InAs diffraction peak in opposite directions, and the composition of the resulting quaternary In(Ga)As(Sb) compound can thus not be fully evaluated by HR-XRD alone, but additional photoluminescence measurements are required.

We also scanned the InAs surface with AFM to evaluate the surface morphology. The rms values for the InAs films grown on the optimized buffers were found to be lower than 7 nm, which is similar to values reported by others.¹⁶ However, no clear dependence of rms roughness versus buffer thickness was obtained. Despite that the InAs growth mitigates the terraces, forming around the screw dislocations as shown in Fig. 3(b), the screw dislocations from the GaSb buffer are still visible in the AFM images. We note that the screw dislocation density remains similar for samples with different buffer layer thicknesses. An additional vertical structure appeared on these InAs/GaSb heterostructures. These could be related to locally affected InAs growth due to the presence of a threading dislocation in agreement with recent MBE studies.¹⁷

To characterize the GaSb layers electrically we removed the InAs layer on one set of samples by selective wet etching using a citric acid:H₂O₂ solution (1:1). Van der Pauw–Hall measurements were performed on the remaining GaSb buffer layer and the results are shown in Fig. 3(b), where the GaSb mobility increases with increasing buffer thickness, supporting

the XRD results. The 1.3- μm -thick GaSb buffer exhibited a mobility of 620 $\text{cm}^2/\text{V s}$ and a hole concentration of $3.6 \times 10^{16} \text{ cm}^{-3}$ at room temperature. At 77 K, the mobility increased to 3000 $\text{cm}^2/\text{V s}$ and the carrier concentration was $9.2 \times 10^{15} \text{ cm}^{-3}$. These values are comparable to other reported results.^{6,8,10} Due to the Sb carryover it is possible that a thin layer of InAs remains after the selective InAs etch. To minimize its effect, measurements by a profilometer are used to verify that the complete layer (23 nm thick) is etched away. Therefore, any residual InAs will have only minor influence on the measured values.¹⁸

C. Electrical evaluation of InAs membranes

Detailed analysis of the Hall measurement data obtained from InAs film grown GaSb buffers is complicated by the parallel hole current that is always present in the GaSb buffer. Therefore, we have formed InAs membranes on a second set of samples by a combination of electron beam lithography and selective wet etching of the underlying GaSb layer (NH₄:H₂O 1:4), as shown in Fig. 4(a). Both Hall devices and two terminal devices of various lengths were made from free-standing InAs membranes with a thickness of 23 and 90 nm, respectively, grown on 1.3- μm -thick GaSb buffer layers. The width of the membranes was chosen to be 4 μm , allowing the measurement of a Hall voltage modulation with magnetic field strength, as shown in the inset of Fig. 4(b). The extracted mobilities of InAs membranes are shown in Fig. 4(b). The 90-nm-thick membranes show a mobility of about 3000 $\text{cm}^2/\text{V s}$ at room

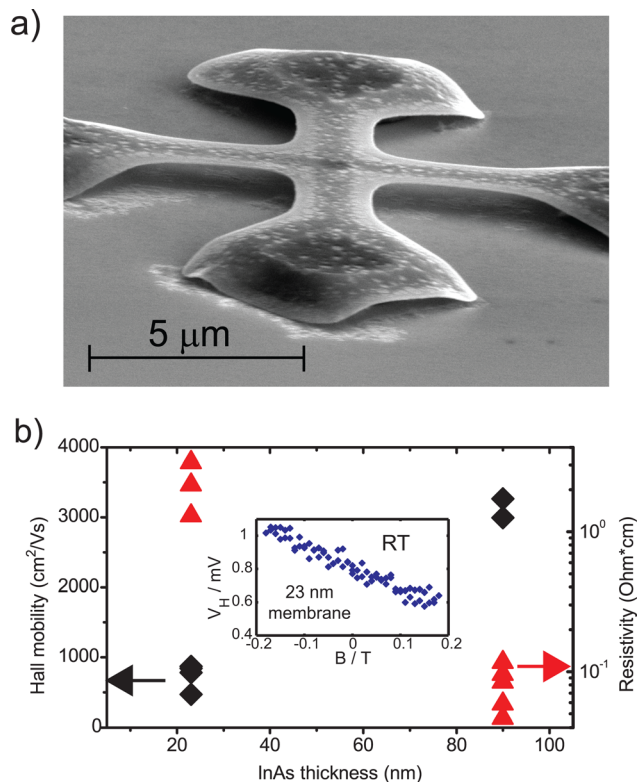


FIG. 4. (Color online) (a) SEM image of under-etched membrane for Hall measurements. (b) Hall mobility and resistivity of under-etched InAs membranes. The inset shows the Hall voltage change with magnetic field for the 23-nm-thick membrane. The current is set to 1 μA .

temperature and an electron concentration of $1.1 \times 10^{17} \text{ cm}^{-3}$. The mobility for the thinner (23-nm-thick) membranes are about $750 \text{ cm}^2/\text{V s}$. It is worth noting that these values are measured using Hall measurements, while most evaluations for InAs nanostructures are made using the field effect, a method that is more sensitive to series resistances in the structures. The increase in resistance for the 23-nm-thick InAs membranes may be related to quantum confinement that reduces the number of available states for carrier transport. We calculated a 100 meV separation between quantized subbands for the 23-nm-thick InAs quantum well with infinite potential walls. This separation energy is four times larger than the thermal excitation and could thus contribute to the increase in the membrane resistance. In fact, early results for InAs nanowire transistors showed an increasing threshold voltage for thinner wires consistent with the confinement model.¹⁹ However, the larger surface-to-volume ratio of the thinner membranes also makes them more sensitive to processing-induced surface effects, which may affect both scattering and the position of the surface potential. It has, for instance, been observed that the field-effect mobility of InAs nanowires is reduced for diameters corresponding to the dimensions studied here.²⁰ We would like to mention that the membranes were passivated with NH_4S_x solution before measurements. Without passivation, no Hall voltage modulation is observed in the 23-nm-thick InAs membranes. This result agrees well with a study of InAs nanoribbons that also observes a clear influence of the surface treatment on the resistance in thin InAs layers.²¹ While it is generally concluded that the InAs surface is pinned within the conduction band, we cannot rule out the possibility that the surface potential also is affected by the processing conditions, where small adjustments of the pinning energy may lead to large effects due to the large surface-to-volume ratio for these nanostructures.

To verify our results from the Hall measurements, we varied the membrane length between 5 and $35 \mu\text{m}$ in order to measure the two terminal membrane resistivity by a transmission line method. As shown in Fig. 4(b), the resistivity of 23-nm-thick InAs membranes is higher than the resistivity of the 90-nm-thick membranes by about 1 order of magnitude. In agreement with the above-presented discussion about the Hall data, we mainly attribute the high resistivity of 23-nm-thick InAs membranes to a stronger influence of the surface.

IV. SUMMARY AND CONCLUSIONS

The growth conditions for thin GaSb buffer layers were optimized and the structural quality and electrical properties were evaluated. The optimal growth conditions for the GaSb buffer layer were found to be a growth temperature of 570°C and a V/III ratio of 3, with a thin nucleation layer grown at 450°C . We also showed that both the electrical and structural quality of the GaSb buffer quality increase with increasing thickness. Screw dislocations are observed for all samples, but their density does not appear to be limiting the layer quality.

We have integrated an InAs layer onto the GaSb buffer layer and observed a direct relation between the quality of

the GaSb buffer and the InAs layer. A gradual improvement in the structural quality of both layers was observed with increasing GaSb thickness up to $1.3 \mu\text{m}$. The mobility of the GaSb layer correlates directly with the XRD peak FWHM value, and a higher buffer layer quality results in better electrical properties. We also observe that the structural quality of the InAs is directly proportional to the GaSb quality. The FWHM value of the InAs layer is 100 arcsec higher compared to the GaSb buffer layer, explained by the high level of lateral strain in these thin films.

We fabricated and measured Hall effect of InAs membranes and show that 23-nm-thick InAs membranes have lower Hall mobility than 90-nm-thick InAs membranes. The 23-nm-thick membranes are sensitive to surface passivation treatment; therefore the low mobility compared to bulk InAs is attributed to surface scattering, while thicker 90 nm membranes are less sensitive to surface effects. These results reveal the challenges involved in realizing and characterizing thin film InAs devices, and especially highlight the importance of the InAs surface for the measured conductivity.

ACKNOWLEDGMENTS

This work was supported by the Swedish Research Council (VR), the Swedish Foundation for Strategic Research (SSF), Knut and Alice Wallenberg Foundation (KAW), and the Nanometer Structure Consortium at Lund University (nmC@LU).

- ¹A. Lubow, S. Ismail-Beigi, and T. P. Ma, *Appl. Phys. Lett.* **96**, 122105 (2010).
- ²D.-H. Kim and J. A. del Alamo, *IEEE Electron Device Lett.* **31**, 806 (2010).
- ³U. Singiseti *et al.*, *IEEE Electron Device Lett.* **30**, 1128 (2009).
- ⁴Li Ning, E. S. Harmon, J. Hyland, D. B. Salzman, T. P. Ma, and P. D. Ye, *Appl. Phys. Lett.* **92**, 143507 (2008).
- ⁵K. G. Eyink *et al.*, *J. Appl. Phys.* **104**, 074901 (2008).
- ⁶C. A. Wang, S. Salim, K. F. Jensen, and A. C. Jones, *J. Cryst. Growth* **17**, 55 (1997).
- ⁷X. B. Zhang, J. H. Ryou, R. D. Dupuis, A. Petschke, S. Mou, S. L. Chuang, C. Xu, and K. C. Hsieh, *Appl. Phys. Lett.* **88**, 072104 (2006).
- ⁸M. Lakrimi, R. W. Martin, N. J. Mason, R. J. Nicholas, and P. J. Walker, *J. Cryst. Growth* **110**, 677 (1991).
- ⁹S. K. Haywood, R. W. Martin, N. J. Mason, and P. J. Walker, *J. Cryst. Growth* **97**, 489 (1989).
- ¹⁰P. Y. Wang, J. F. Chen, and W. K. Chen, *J. Cryst. Growth* **160**, 241 (1996).
- ¹¹M. Lakrimi, R. W. Martin, N. J. Mason, R. J. Nicholas, and P. J. Walker, *J. Cryst. Growth* **124**, 395 (1992).
- ¹²S. G. Ghalamestani, M. Berg, K. A. Dick, and L.-E. Wernersson, *J. Cryst. Growth* **332**, 12 (2011).
- ¹³R. People and J. C. Bean, *Appl. Phys. Lett.* **47**, 322 (1985).
- ¹⁴D. Lackner *et al.*, *J. Cryst. Growth* **311**, 3563 (2009).
- ¹⁵J. Steinschneider, J. Harper, M. Weimer, C.-H. Lin, S. S. Pei, and D. H. Chow, *Phys. Rev. Lett.* **85**, 4562 (2000).
- ¹⁶A. A. Khandekar, G. Suryanarayanan, S. E. Babcock, and T. F. Kuech, *J. Cryst. Growth* **292**, 40 (2006).
- ¹⁷G. Moschetti *et al.*, *Appl. Phys. Lett.* **97**, 243510 (2010).
- ¹⁸R. L. Petritz, *Phys. Rev.* **110**, 1254 (1958).
- ¹⁹C. Thelander, M. T. Bjork, M. W. Larsson, A. E. Hansen, L. R. Wallenberg, and L. Samuelson, *Solid State Commun.* **131**, 573 (2004).
- ²⁰A. C. Ford, J. C. Ho, Y.-L. Chueh, Y.-C. Tseng, Z. Fan, J. Guo, J. Bokor, and A. Javey, *Nano Lett.* **9**, 360 (2009).
- ²¹H. Ko *et al.*, *Nature (London)* **468**, 286 (2010).